Journal of Materials Chemistry

Cite this: J. Mater. Chem., 2011, 21, 16049

www.rsc.org/materials

PAPER

Enhanced gas sensing performance of TiO_2 functionalized magneto-optical SPR sensors †

M. G. Manera,*[a] G. Montagna,[a] E. Ferreiro-Vila,[b] L. González-García,[b] J. R. Sánchez-Valencia,[c] A. R. González-Elipe,[c] A. Cebollada,[b] J. M. Garcia-Martin,[b] A. Garcia-Martin,[b] G. Armelles[b] and R. Rella[a]

Received 3rd May 2011, Accepted 9th August 2011
DOI: 10.1039/c1jm11937k

Porous TiO_2 thin films deposited by glancing angle deposition are used as sensing layers to monitor their sensing capabilities towards Volatile Organic Compounds both in a standard Surface Plasmon Resonance (SPR) sensor and in Magneto-Optical Surface Plasmon Resonance (MO-SPR) configuration in order to compare their sensing performances. Here our results on the enhanced sensing capability of these TiO_2 functionalized MO-SPR sensors with Au/Co/Au transducers with respect to traditional SPR gas sensors are presented.

Introduction

Surface plasmon resonance (SPR) is a surface-sensitive analytical technique used in a variety of chemical and biological sensors.[1–4] Surface plasmon polaritons (SPPs) are essentially collective charge density oscillations bound to a metal–dielectric interface that can be excited on thin metal films for example through gratings or prism couplers. When excited, such collective oscillations of conduction electrons create regions of enhanced electromagnetic (EM) fields in the direct proximity of the metal surface that are extremely sensitive to the local changes of refractive index occurring at the surface of the thin metal film, which in turn provides a capability for a label-free form of analytical detection.[5] As a result, this technique is widespread used to monitor the binding of biomolecules to the Au or Ag surface, as well as to monitor interactions between biomolecules of different nature in the nanomolar to picomolar range, in real time. Applications of this technology can be found in biology, food safety, medical diagnostics and environmental monitoring.[6–10]

The main problem of such SPR technology in commercially available systems is associated with the existence of a lower physical limit of detection (LOD) with respect to fluorescence approaches which however need a further labelling step. This limit is conditioned by the level of noise in measurements.

Apart from the slight improvements offered by the optimization of the optical metrology systems and the use of more efficient data analysis methods, various approaches have been proposed to enhance the sensitivity of such techniques. These include, for example, phase-sensitive detection schemes, azimuthal control of grating coupled SPR, use of metallic nanostructures such as metal nanoparticles, line gratings, or hole arrays in metal films, structures that each provide an efficient coupling mechanism through which to excite plasmons, *etc.*[11–16]

In this context, modulation techniques can be used to improve the signal to noise ratio (SNR) and enhance the limit of detection. Lock-in amplifiers use a technique known as phase-sensitive detection to single out the component of the signal at a specific reference frequency and phase.

Recently research in the plasmonics field is going to move into active plasmonics, proposing to add active functionalities to these SP-based devices. The development of active plasmonics requires the use of novel materials in which the surface plasmon properties can be controlled by an external agent. Different control agents have been proposed in the literature: temperature,[17] electric field,[18] electromagnetic waves[19] or magnetic fields.[20,21] In fact, the latter is what happens in the magneto-plasmonic system, *i.e.* structures exhibiting high magneto-optical (MO) activity and intense plasmonic resonances. The MO activity consists of the interaction between linearly polarized light and magnetized matter, and depending on the relative orientation between the plane of incidence and the magnetization, different effects can take place. For instance, in the transverse MO Kerr effect (TMOKE), the magnetization lies in the sample plane but is perpendicular to the plane of incidence of p-polarized light, and the intensity of the reflected light depends on the magnetization.

The application of the idea of the magneto-plasmonic effect has been shown to bring about an enhancement of their MO response upon plasmon excitation in surface plasmonic crystals[21]

[a]*CNR-IMM-Institute for Microelectronic and Microsystems, unit of Lecce, Via Monteroni, 73100 Lecce, Italy. E-mail: mariagrazia.manera@le.imm.cnr.it*
[b]*IMM-Instituto de Microelectrónica de Madrid (CNM-CSIC), Isaac Newton 8, 28760 Tres Cantos, Madrid, Spain*
[c]*Instituto de Ciencia de Materiales de Sevilla (CSIC-Univ. Sevilla), Avda. Américo Vespucio 49, 41092 Sevilla, Spain*
† Electronic supplementary information (ESI) available. See DOI: 10.1039/c1jm11937k

and to modify the propagation of surface plasmon waves. This has been demonstrated in ferromagnetic wires,[22,23] where it has been shown that the excitation of a plasmon running along the wire gives rise to an enhancement of the magneto-optical response.

Although the MO activity is very high in ferromagnetic materials, as for instance Fe, Ni and Co, such materials suffer from strong plasmon damping. So, the best magnetoplasmonic performance is obtained in metallic heterostructures made of noble metals and ferromagnetic materials, since they can sustain intense surface plasmons and have at the same time high magneto-optical activity.

Very recently, a MOSPR sensor, based on the combination of magneto-optic effects and SPR, has been proposed.[24] This sensor is based on a magneto-plasmonic (MP) modulation technique produced in multilayers of noble and ferromagnetic metals. This combination has shown a great enhancement of MO Kerr effects of p-polarized light when the surface plasmon resonance condition is satisfied. Such enhancement strongly depends on the excitation conditions of the SPP and therefore on the refractive index of the dielectric in contact with the metal layer, thus providing the sensing principle for the MO-SPR device. If in the traditional SPR sensor, the metal layer (usually Au) acts as the transducing layer, in this case it is represented by the MP multilayer structure combining noble metal and ferromagnets with a suitable thickness. In Fig. 1 a sketch of a typical experimental setup with a test chamber for gas sensing is shown.

For the specific gas sensing application of SPR, an "active sensing layer" is needed onto the Au or Ag transducing substrate. Its active role consists of the change of its optical constants upon the interaction with the investigated gas which can be sensitively detected as a change in the reflectivity SPR curve. Obviously, a porous sensing layer is highly desirable since it provides a large surface area to be put in contact with the gaseous ambient to be monitored. Organic, inorganic or mixed active sensing materials can be chosen, with various structural and morphological features for these purposes.[25–27] Also, nanostructured semiconductor metal oxides, such as SnO_2, ZnO, TiO_2, and NiO, are promising sensing materials for a wide range of gases and vapours. The enhanced sensing features are determined by the high chemical activity and porosity of the active materials, which are direct consequences of their nanostructure. Because of this, gas sensing capabilities depend critically on the synthesis method and parameters that allow for tailoring of selectivity and sensitivity toward the target species.

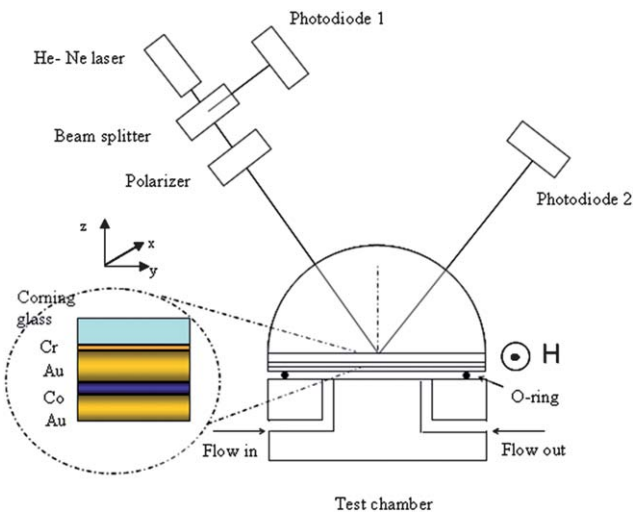

Fig. 1 Experimental setup for SPR and MO-SPR gas sensing.

In this work a novel application of such MO-SPR sensors is proposed in chemical gas sensing purposes. Thin films of nanoporous columnar TiO_2 deposited by glancing angle deposition (GLAD) have been chosen as sensing material to detect the presence of different alcohol vapours of interest in food applications. GLAD is a physical vapour deposition method capable of producing thin films with a highly porous nanostructure that can be tuned to meet the needs of different applications.[28,29] During deposition, the zenithal angle α (angle of vapour incidence) and the azimuthal angle ϕ (angle of substrate rotation around the substrate normal) are adjusted in response to real-time measurement of vapour deposition rates to yield a specific film nanostructure. The enhanced surface area observed in GLAD films has been exploited in a variety of applications particularly in fabricating sensor devices.[30,31] Due to their inherently porous nature, gaseous species in the ambient environment are free to diffuse through the structure producing detectable changes in the dielectric constant of the system.[29] Moreover, the inner surface of the oxide films (such as SiO_2, TiO_2, and Al_2O_3) fabricated using GLAD may promote the capillary condensation of water vapour within the porous structure, and thus be used for humidity sensors.[32]

The aim of this work is to propose a novel combination of materials based on TiO_2 thin films deposited by GLAD onto Au/Co/Au multilayers with optimized thicknesses to act as the transducer element in MO-SPR gas sensors. We will demonstrate its sensing performance by testing it against different alcohol vapours, finding superior sensitivity values than the traditional SPR sensors.

The novelty of the presented work comes from the combination of transducing (a multilayer structure composed of noble and ferromagnetic metals) and sensing (porous TiO_2 materials) layers; the first endorses active plasmonic functionalities, while the second takes advantage of their porous nature, to give rise to a system with great gas sensing performance. Therefore mastering the deposition process will allow sensing functionalities to be further enhanced.

Experimental details

Preparation of magneto-optical transducing layers

A set of 15 nm Au/6 nm Co/25 nm Au/2 nm Cr multilayers were deposited on Corning glass substrates. The 2 nm thick Cr layer between the substrate and the 25 nm Au layer improves the adherence of the magnetoplasmonic structure. All layers were deposited by dc magnetron sputtering at room temperature in an ultrahigh-vacuum chamber with a base pressure of 10^{-9} mbar. In these conditions all the constituent layers are polycrystalline and the Co layer has in-plane magnetization.

The choice of these thickness values comes from the need to prevent Co oxidation while maximizing the magneto-optical ΔR signal upon the change in the real part of refractive index n.[20]

TiO_2 sensing layers deposition

Once the transducer layers are grown, they were transferred to a different deposition system where a 10 nm amorphous TiO_2 thin film was deposited on top by using the glancing-angle deposition (GLAD) technique. Reference TiO_2 layers were also grown onto Au/Cr/glass and bare glass substrates. The porous nanocolumnar layer of TiO_2 was grown by electron beam evaporation from a TiO source under a residual oxygen pressure of 5×10^{-4} Torr at a zenithal angle of incidence of 70°. No rotation around the azimuthal angle was intended for the prepared films which, in this way, presented a tilted columnar nanostructure.[29] The deposition rate and film thickness were controlled with a calibrated quartz crystal monitor placed at a normal angle besides the substrates. Further details on the deposition process and optical features of the realized materials can be found in ref. 29.

Characterizations

The morphology of the TiO_2 thin films deposited both onto the bare glass substrates and onto the Au/Co/Au multilayers was investigated by Atomic Force Microscopy (AFM) in dynamic mode using probes with about 5 N m^{-1} force constant and 7 nm tip radius.

Optical characterization of the TiO_2 thin films deposited onto the Au/Co/Au multilayer and onto glass was carried out using spectral ellipsometry, allowing the effective refractive index of the investigated TiO_2 thin films to be extracted. In both cases, a refractive index of 1.682 was obtained at 632.8 nm wavelength, which is significantly smaller than that of bulk TiO_2 (2.494). This value is in agreement with previously reported refractive indexes of TiO_2 thin films prepared by GLAD[29] and indicates that these films are very porous. *Details can be found in the ESI*†. The magnetic field needed to saturate the Co layer of the transducer (30 Oe) was determined by TMOKE hysteresis loops, *i.e.* measuring the in-plane magnetization reversal.

For these structures the optical and magneto-optical characterizations consist of measurements of reflectivity and transverse Kerr signal $\Delta R/R$ *versus* incident angle in the Kretschmann configuration at a wavelength of 632 nm.

Traditional SPR and MO-SPR measurements were performed in a home-made experimental set-up using Kretschmann's prism configuration as shown in Fig. 1. The free face of the glass substrate was brought into optical contact with a prism (with refractive index $n = 1.515$, determined by Brewster angle measurement) using a thin layer of an index-matching fluid ($n = 1.517$). The prism/sample combination was placed on a θ–2θ rotation table driven by a microprocessor-controlled stepping motor (with a resolution of 0.01°). Surface plasmon excitation was achieved by focusing a p-polarized light beam of a He–Ne monochromatic laser source ($\lambda = 632.8$ nm) onto the prism/sample interface. The reflected light is detected by a Si photodiode.

To explore the modulation of the surface plasmon wavevector by an external magnetic field, an electromagnet was placed in transversal configuration, *i.e.* it produces a magnetic field that lies in the plane of the Co layer and perpendicular to the incidence plane, which changes the magnetization of the Co layer between its saturation states with a magnetic field of 30 Oe and a frequency of 800 Hz. The modulated signal was processed by a pre-amplifier and then by a lock-in amplifier which will extract the component of the signal at the specific reference frequency rejecting noise. This will allow the variation of the reflectance signal to be obtained upon the modulation of the direction of the magnetic field in the transversal configuration as:

$$\frac{\Delta R}{R} = \frac{R(+M) - R(-M)}{2R(0)} \quad (1)$$

where $R(\pm M)$ and $R(0)$ are the reflectance of the p-polarized light with the sample magnetically saturated along the direction of the applied magnetic field and in the demagnetized state, respectively. The latter is measured before applying the magnetic field.

Sensing characterization

A suitable Teflon SPR test chamber was used in order to analyse the sensing activity of all the deposited TiO_2 nanostructured thin films. The SPP excitation manifests itself as a reduction on the reflectivity at a specific angle of incidence above the critical angle for total internal reflection.

The sensing performances of the prepared TiO_2 thin films deposited onto Au and Au/Co/Au substrates were investigated towards different concentrations of ethanol, methanol and isopropanol vapours mixed in dry-air as carrier gas. The investigated analytes were introduced into a 20 mL vial kept at room temperature by a thermostatic tank. To evaluate the optical sensor response towards the investigated alcohol vapours present in the head space of the vial, a dry air flow (total flow of 50 sccm) was deviated in the vial for collecting the analysed saturated vapour. The obtained concentration of the saturated vapours depends on their saturated vapour pressure and the temperature at which the sample is kept. The maximum vapour concentration C_{max} formed in a closed test chamber can be calculated by dividing the vapour pressure at a given temperature by the atmospheric pressure. For example, at 25 °C the methanol vapour pressure is $p_{25} = 16.9$ kPa and the maximum vapour concentration is:

$$c_{max} = \frac{p_{25}}{p_{atm}} \times 100 = 16.6 \times 10^4 \text{ ppm}$$

To obtain different concentrations of the analyte vapours sent in the test chamber, the air flow carrying the saturated vapours was diluted to the reference flow of dry air in different suitable ratios for each alcohol vapour. The gas mixing station consists of a mass flow controller (MKS Instruments model 647B) equipped with two mass flow/meters/controller (MFCs) and a system of stainless steel pipelines and switching valves. The experimental procedure started by flowing dry air through the sample chamber until a steady absorbance reading was obtained. Next, fixed concentrations of vapours were transferred into the sensor test cell realized in the meander pipe as described above.

Results and discussions

In Fig. 2 we show AFM images and representative topographical profiles of the 10 nm TiO_2 thin films deposited onto a glass

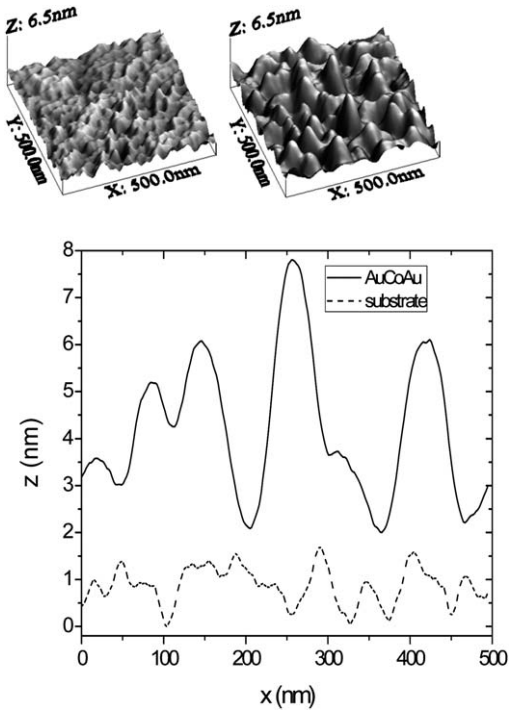

Fig. 2 AFM images of the TiO_2 film onto the substrate (left) and onto the metallic trilayer (right) with representative profiles (lower panel).

substrate and onto the transducing trilayer. Although convolution effects with the AFM tip prevent quantitative information from being obtained, the porous nature of the TiO_2 layer can be observed. As the roughness of the metallic trilayer is higher than that of the glass substrates, the top TiO_2 layer is rougher when it is deposited onto the trilayer, since the autoshadowing mechanism is more efficient.

From TMOKE loops it was checked that the samples exhibited low saturation field (around 30 Oe), as expected for a Co thin layer of a few nm thick.

In Fig. 3 we show the angular dependence of the reflectivity and the magnetic field induced variation of the reflectivity related

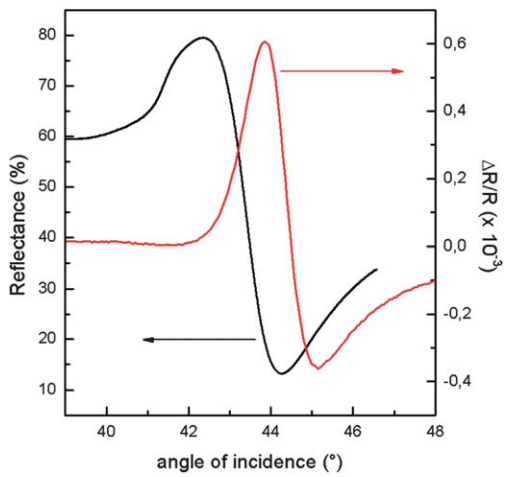

Fig. 3 Reflectivity curve (R *vs.* angle) and TMOKE curve ($\Delta R/R$ *vs.* angle) of Au/Co/Au multilayers deposited on Corning glass substrates.

to total reflectivity ($\Delta R/R$) defined in eqn (1) or the investigated TiO_2/Au/Co/Au sample.

As demonstrated in the literature,[20,24] a magnetic field applied in the plane of a gold–cobalt–gold multilayer film with a cobalt thickness of a few nanometres and perpendicular to the SPP propagation direction induces a modification of the SPP wavevector while keeping its transverse magnetic (TM) character, this modification being the physical origin of the magnetic field induced variation of the reflectivity.

In such a configuration, the dielectric tensor of cobalt (a ferromagnetic metal) is governed by the magnetization M in the plane of the cobalt layer, and so are the properties of surface plasmons at the trilayer–dielectric interface.

The wavevector of such surface plasmon k_{sp} propagating in the y-direction (Fig. 1) depends linearly on the component of the magnetization M_x of the cobalt layer (being maximum at saturation, $M_x = \pm 1$) and exponentially decays as a function of the Co layer thickness below the gold/air interface.[33,34]

In terms of reflectivity, a variation of the plasmon wavevector implies a variation of the angle at which the light–plasmon coupling takes place, so magnetic modulation turns into angular modulation. In other words the Kerr signal in Fig. 3 can directly be related to the angular derivative of the reflectivity signal:[20] $\Delta R/R = (\partial R/\partial\theta)(\Delta\theta/R)$ where $\Delta\theta$ is the angular shift of the reflectivity minimum when the magnetization is reversed.

As shown in Fig. 3, the angular variation of the reflectivity shows firstly the total internal reflection at 42° and then the SPP excitation with the clearly observed minimum around 44.2°. Also the transverse Kerr effect defined as $\Delta R/R$ is characterized by a sharp resonance like angular behaviour at around such a value, *i.e.* when the SPP is excited. When the SPP is not excited, both R and $\Delta R/R$ are basically constant in the same angular range (data not shown).

For the angular positions corresponding to total reflection where the plasmon is not yet excited, the corresponding EM field distribution decreases exponentially from the glass incident light side. However, for angular positions where the SPP has been excited, the EM field gradually increases as the light gets deeper into the structure, reaching as expected a maximum value at the air–Au interface, where the SPP is located. This implies that the EM field is drastically enhanced at the MO-active layer region, being responsible for the enhancement of the magneto-optical signal. Maximal changes in the magneto-optical signal will occur in the dip of the SPR curve where the probing electric field is maximal, whereas maximal reflectivity changes are observed on the resonance slopes.

Under optimal thickness of the MO-supporting structure, the magneto-optical signal can thus provide a better sensitivity to refractive index variations than reflectivity measurements. This expectation is based on the existence of a sharp jump in the angular dependence of the magneto-optical signal under SPR condition, besides the reduced signal noise dictated by the detection scheme which in turn results in a much better signal-to noise ratio.

In Fig. 4 the SPR reflectivity curves for the Au/glass and TiO_2/Au/glass (a) as well as Au/Co/Au/glass and TiO_2/Au/Co/Au/glass (b) are reported. In both cases, when the TiO_2 layer is on top, the incident angle θ_{spr} in which the reflectivity minimum takes place exhibits a shift to higher angles with

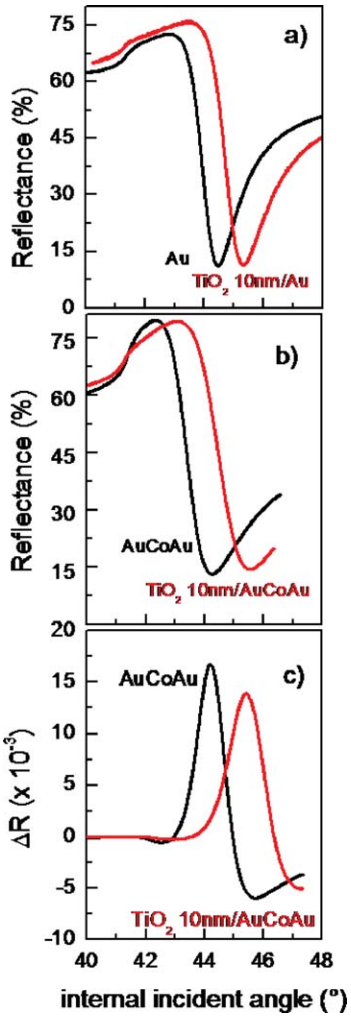

Fig. 4 *R vs.* angle of Au(50 nm)/glass and TiO_2(10 nm)/Au/glass (a), *R vs.* angle of Au/Co/Au/glass TiO_2 (10 nm)/Au/Co/Au/glass (b) and ΔR *vs.* angle of the same samples (c).

respect to the bare metal/glass samples. This difference can be ascribed to a change in the actual refractive index above the gold layer when the metal surface is covered by the TiO_2 film. The shift magnitude in the SPR angle typically depends on both the thickness and the refractive index *n* of the titania deposited layer. It is also worth noticing the broadening of the curve around the minimum in the case of Au/Co/Au, since the presence of a Co layer increases the absorption losses compared to pure Au.

If a magnetic field is applied, ΔR curves will record a change in the angular position when a thin TiO_2 layer is deposited onto the Au/Co/Au multilayers substrate (Fig. 4(c)). Also in this case, this change can be ascribed to the change of refractive index due to the presence of a thin film at the Au/air interface.

Two different sensing approaches can be used to test the ability of the TiO_2 layers to detect the presence of different alcohol vapour molecules such as ethanol, methanol and isopropanol. The realized Au/Co/Au multilayer has been using as transducing layers both in a traditional SPR sensing configuration and in the proposed MO-SPR gas sensor configuration. In the first case, the reflectance of the active sensing layers, recorded in the Kretschmann configuration, is monitored during time, at a fixed angle, corresponding to the maximum slope of the SPR curve reported in Fig. 4(b). In the second case, the ΔR magneto-optical signal, recorded in the presence of the oscillating magnetic field in transversal configuration, is monitored during time, at a fixed angle, corresponding to the maximum slope of the ΔR curve reported in Fig. 4(c). Increasing concentrations of alcohol vapours mixed in dry air were sent into the test chamber, spaced out by a flux of whole dry air with the aim to evaluate the reversibility of the sensors after interaction with the investigated analytes. The interaction of the sensing layer with the alcohol vapours produced a change in the optical properties of the sensing TiO_2 films, namely a change in the refractive index[26] or a swelling mechanism if the alcohol vapours are allowed to penetrate into the porous structure of the sensing layers, which can be responsible for a change in its thickness values. This effect produces a change in the plasmon wavevector, which, in turn, translates into a change in the SPR curve and MO-SPR curve. Thus, the two recorded signals have the role to monitor the optical changes of the TiO_2 active layer upon the interaction with the investigated alcohol vapours.

In Fig. 5 the calibration curves relative to SPR and MO-SPR sensors are reported. The curves put in evidence the obtained sensor responses corresponding to the different alcohol vapours. These curves represent the signal variation in the presence of the analyte and in dry-air with respect to the value of the signal in dry-air. Here the signal is intended as the reflectance signal or magneto-optical ΔR signal for the two different SPR and MO-SPR configurations, respectively. The gas sensing measurements were done in the same experimental setup, with the same sample, and flowing the same alcohol vapour analytes obtained under the same experimental conditions.

Due to the different nature of reflectance measurements in the SPR sensor and of the MO measurements in the MO-SPR sensor, the comparison of their sensing performances, namely of their calibration curves, must be done taking into account the signal-to-noise ratio (SNR) of the experimental measurements. In this sense noise is anything which contributes to the signal but which is not due to the parameter being measured. It is generated in all parts of the electrical circuitry but in light measurement systems it is dominated by noise from the detector or from the optical signal. As in a first approximation the SNR depends on the square root of the frequency, the modulation of the MO signal at 800 Hz improves the MO measurements filtering the noise. The system noise here is defined as the RMS deviation of the experimental signal (during 1000 s) when dry air flows in the test chamber. The limit of detection would be five times the system noise (Rose criterion).

Sensitivity information can be obtained by the slope of the calibration curves.[35] The experimental results yield a significant enhancement of the MO-SPR sensor sensitivity towards the investigated alcohol vapours with respect to the intensity-interrogated SPR sensor, using the same Au/Co/Au layer as sensing transducer, as can be noticed in Table 1.

For the sake of completeness, the sensing performances of the TiO_2 active layers were investigated in a "traditional" SPR configuration using as transducing layer the traditional Au/glass substrates (in the optimal configuration 48 nm Au/2 nm

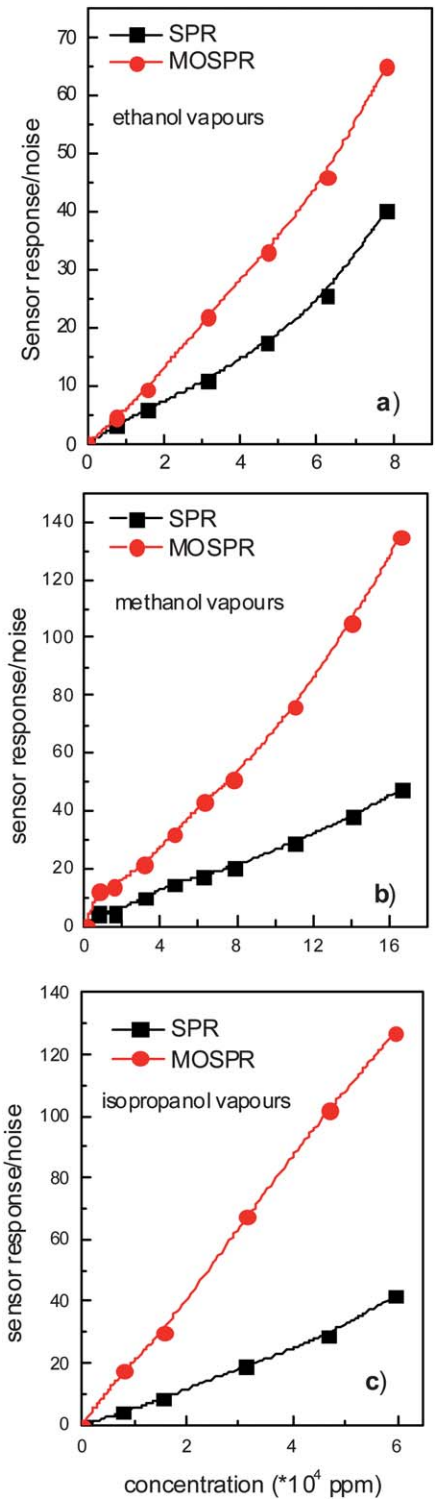

Fig. 5 Calibration curves relative to ethanol vapours (a), methanol vapours (b) and isopropanol vapours (c).

Cr/glass). Both Au/glass and Au/Co/Au/glass structures were deposited on the same kind of Corning glass substrates, using the same growth conditions, as well as the same TiO_2 sensing layer deposited on them. The obtained sensitivity results are reported in Table 1 with the name "traditional SPR".

Table 1 Sensitivity comparison (ppm^{-1})

	Transducing layer		
	Au/Co/Au		Au
Analyte	MO-SPR sensor ($\times 10^{-4}$)	SPR sensor ($\times 10^{-4}$)	Traditional SPR sensor ($\times 10^{-4}$)
Ethanol	7.2	3.6	6.0
Methanol	7.8	2.8	4.2
Isopropanol	21.9	6.3	16.0

Under the same conditions of the sensing technique, the highest sensitivity is obtained for isopropanol vapours. This result agrees with the higher refractive index of isopropanol (*i.e.*, 1.380) with respect to that of methanol (*i.e.*, 1.329) and ethanol (*i.e.*, 1.361) and by the steric hindrance of its molecules with respect to other vapours: this allows a fast and complete coverage of the surface, thus leading to reach quickly a saturation level in the sensor signal as well as to penetrate and diffuse into the TiO_2 matrix leading to a change in the density and thus in the refractive index of the active layer.

But if we compare the sensitivity recorded by the different sensing techniques, methanol vapour is the analyte which gives a higher enhancement in the performance of MO-SPR sensing compared to a traditional SPR sensor device. In order to justify this result, we have to take into account that the values reported in the table represent the sensitivity that is the speed at which the sensor signal changes upon a variation of the analyte concentration. As known from SPR theory, a variation in the dielectric constant ε_d of the medium in contact with the Au/air interface upon the change in the refractive index causes a variation in the plasmon wavevector k_{sp} due to its direct dependence on ε_d. The electromagnetic field exponentially decaying at the Au/air interface became therefore a sensing probe for changes of the refractive index at this interface, translating into a variation of the SPR signal. The rapidity of this variation depends on the capacity of the wavevector to follow the changes at the transducer interface, which in turn depends on the ability of the decaying field to penetrate into the dielectric and to follow the changes of its optical parameters.

In the MOSPR signal the plasmon wavevector k_{sp} direction is modulated at a certain frequency by the modulation of the magnetization in the plane of the Co layer. The modulated wavevector Δk is now responsible for the detection of refractive index changes at the Au/air interface. The capacity of the modulated wavevector to follow such optical variations dictates the sensitivity with respect to the different analytes. A small gas molecule such as methanol will allow the electromagnetic field to follow better the changes in gas concentration resulting in a faster change in Δk with respect to bulky analyte molecules such as isopropanol. In addition, small analyte molecules will interact with the sensing layer in proximity of the MO active layer region where the electromagnetic field, responsible for the enhancement of the magneto-optical signal, is drastically enhanced allowing a fast probing of analyte changes.

These considerations come from the comparison of traditional SPR and MOSPR configurations using Au film and Au/Co/Au multilayer films as transducing layers respectively. In the two

cases the probing electromagnetic field at the metal/air interface is the best for each experimental sensing configuration. As shown in the table, a reduction of sensitivity towards methanol vapours of the SPR sensor using Au/Co/Au as transducing layer with respect to the traditional SPR sensor is obtained. This can be ascribed to the reduced probing ability of the decaying electromagnetic field at the Au/air interface, due to a damped plasmon excitation in the Au/Co/Au structure with respect to the classical Au/air interface. This is why considering the SPR and MOSPR detection in the same support (Au/Co/Au), the above considerations about methanol vapours are not valid since in this case isopropanol vapour reports the highest sensitivity.

The comparison of sensitivity values obtained for the investigated transducing sensor platforms highlights the significant and important enhancement obtained with the MO-SPR sensor over the traditional SPR approach, confirming the hypothesis outlined by the authors at the beginning of the work.

Dynamic curves relative to the analyte reporting the best sensing performance, namely isopropanol vapours, are reported in Fig. 6 as representative of the behaviour of all tested alcohol vapours. The stability of the signal and reversibility in the absorption and desorption processes are observed in all the concentration range and for all investigated analytes for the two SPR and MO-SPR configurations. A large increase in the signal is observed in the sensorgram corresponding to MO-SPR measurements, thus confirming the achieved objective of this work. However, this configuration presents a slight reduction in the recovery times as can be noticed in the figure. Reproducibility of the measurements is ensured by repeating the measurements for more cycles.

The assumed interaction of the investigated alcohol vapours with the TiO_2 sensing layers is likely due to the physical adsorption into the sensing layer. Indeed, the calibration curves follow an analytical behaviour typical of a sigmoid isotherm (often named Type II isotherm).[36,37] This isotherm is characteristic of weak gas–solid interactions and it usually corresponds to multilayer formation. Once the target analyte approaches the film, a specific equilibrium should set in, involving the reversible condensation of the alcohol vapour molecules into the porous structure of the TiO_2 film. Once the first monolayer of the vapour molecules has become adsorbed in the inner surface of the layer, it will form multilayers up to completely filling the pores and the resulting isotherms will become convex to the concentration, or better to the pressure axis. This effect is less evident in isopropanol vapours; we stress that this behaviour is due to the lower polarity of their molecules.

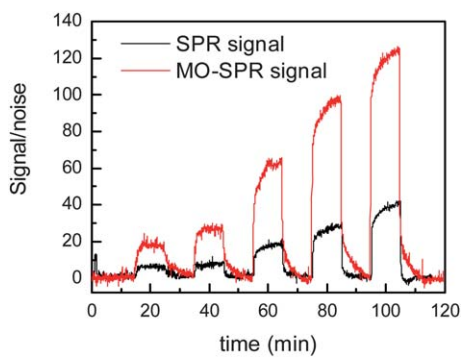

Fig. 6 Dynamic curves (R and ΔR *vs.* time) of isopropanol vapours at different concentrations (both R and ΔR).

The layer with their pores completely filled with the vapour molecules will undergo a sharp change in the overall refractive index of the film and, in turn, to the corresponding modification in the SPR response. By assuming a similar degree of filling of the pores for the three investigated vapours, it is likely that the magnitude of the change depends on the refraction index of the three analytes (*i.e.*, 1.380, 1.361 and 1.329 for isopropanol, ethanol and methanol).

These considerations are not in contrast with the above observations about sensitivity comparison, because sensitivity is determined taking into account the linear part of the calibration curves corresponding to lower concentrations. The multilayer behaviour is noticed taking into account the higher concentrations of vapours analytes.

The physisorption character of the interaction of the analytes with the TiO_2 pore surfaces ensures the reversibility of the sensing mechanism. Measurements of the TiO_2 thin films active layer (deposited by the GLAD technique) with higher thickness will be performed. We expect that this deposition technique would likely produce higher porosity in a thicker sensing film whose expected sensing performance would be consequently higher.

By comparing the obtained results with other studies on SPR gas sensing using TiO_2 prepared by different routes,[38,39] we can conclude that the discussed work represents a step forward in SPR technology as concerns gas sensing, building a bridge between the sensor and magnetic community and paving the way for the study of other active plasmonic functionalities for gas or biosensing applications.

Conclusions

We have presented a novel combination of materials, namely a magnetoplasmonic Au/Co/Au trilayer with a TiO_2 layer deposited on top by GLAD, and demonstrated their surpassing capabilities as gas sensors by magneto-optical surface plasmon resonance measurements. This has been carried out by evaluating the sensing performance of a thin TiO_2 layer deposited onto both Au and Au/Co/Au substrates to the exposure of different alcohol vapours. A significant enhancement in sensitivity has been found in the MO-SPR sensor with respect to the classical SPR measurements carried out in the intensity-based configuration.

Acknowledgements

This work has been funded by the European Commission (NMP3-SL-2008-214107-Nanomagma), the Spanish MICINN (CSD 2008-00023, MAT 2008-06765-C02-01/NAN, MAT2010-21228), CSIC (JAE fellowship for E. F.-V.) and Comunidad de Madrid (S2009/MAT—1726, S2009/TIC—1476).

Notes and references

1 J. N. Anker, W. P. Hall, O. Lyandres, N. C. Shah, J. Zhao and R. P. Van Duyne, *Nat. Mater.*, 2008, **7**, 442.
2 J. Homola, *Chem. Rev.*, 2008, **108**, 462.

3 D. G. Myszka and R. L. Rich, *Pharm. Sci. Technol. Today*, 2000, **3**, 310.
4 P. H. Rogers, G. Sirinakis and M. A. Carpenter, *J. Phys. Chem. C*, 2008, **112**, 8784.
5 M. Piliarik, H. Vaisocherová and J. Homola, *Methods Mol. Biol.*, 2009, **503**, 65.
6 M. Piliarik, M. Bocková and J. Homola, *Biosens. Bioelectron.*, 2010, **26**, 1656.
7 F. Fernández, K. Hegnerová, M. Piliarik, F. Sanchez-Baeza, J. Homola and M. P. Marco, *Biosens. Bioelectron.*, 2010, **26**, 1231.
8 J. Spadavecchia, M. G. Manera, F. Quaranta, P. Siciliano and R. Rella, *Biosens. Bioelectron.*, 2005, **21**, 894.
9 J. Hottin, J. Moreau, G. Roger, J. Spadavecchia, M. Millot, M. Goossens and M. Canva, *Plasmonics*, 2007, **2**, 201.
10 S. Herminjard, L. Sirigu, H. P. Herzig, E. Studemann, A. Crottini, J. Pellaux, T. Gresch, M. Fischer and J. Faist, *Opt. Express*, 2009, **17**, 293.
11 S. Y. Wu, H. P. Ho, W. C. Law, C. Lin and S. K. Kong, *Opt. Lett.*, 2004, **29**, 2378.
12 P. P. Markowicz, W. C. Law, A. Baev, P. N. Prasad, S. Patskovsky and A. Kabashin, *Opt. Express*, 2007, **15**, 1745.
13 F. Romanato, K. H. Lee, H. K. Kang, G. Ruffato and C. C. Wong, *Opt. Express*, 2009, **17**, 12145.
14 W. L. Barnes, W. A. Murray, J. Dintinger, E. Devaux and T. W. Ebbesen, *Phys. Rev. Lett.*, 2004, **92**, 107401.
15 T. W. Ebbesen, H. J. Lezec, H. F. Ghaemi, T. Thio and P. A. Wolff, *Nature*, 1998, **391**, 667.
16 L. J. Sherry, S.-H. Chang, G. C. Schatz, R. P. Van Duyne, B. J. Wiley and X. Younan, *Nano Lett.*, 2005, **5**, 2034.
17 T. Nikolajsen, K. Leosson and S. I. Bozhevolnyi, *Appl. Phys. Lett.*, 2004, **85**, 5833.
18 M. J. Dicken, L. A. Sweatlock, D. Pacifici, H. J. Lezec, K. Bhattacharia and H. A. Atwater, *Nano Lett.*, 2008, **8**, 4048.
19 D. Pacifici, H. J. Lezec and H. A. Atwater, *Nat. Photonics*, 2007, **1**, 402.
20 J. B. Gonzalez-Diaz, A. García-Martín, G. Armelles, J. M. García-Martín, C. Clavero, A. Cebollada, R. A. Lucaszew, J. R. Skuza, D. P. Kumah and R. Clarke, *Phys. Rev. B: Condens. Matter Mater. Phys.*, 2007, **76**, 153402.
21 G. A. Wurtz, *New J. Phys.*, 2008, **10**, 105012.
22 S. Melle, J. L. Menéndez, G. Armelles, D. Navas, M. Vázquez, K. Nielsch, R. B. Wehrspohn and U. Gösele, *Appl. Phys. Lett.*, 2003, **83**, 4547.
23 J. B. Gonzalez-Diaz, A. García-Martín, G. Armelles, D. Navas, Manuel Vázqez, K. Nielsch, R. B. Wehrspohn and U. Gösele, *Adv. Mater.*, 2007, **19**, 2643.
24 B. Sepulveda, A. Calle, L. M. Lechuga and G. Armelles, *Opt. Lett.*, 2006, **8**, 1085.
25 M. G. Manera, L. Valli, S. Conoci and R. Rella, *J. Porphyrins Phthalocyanines*, 2009, **13**, 1140.
26 H. Denga, D. Yanga, B. Chena and C. Linb, *Sens. Actuators, B*, 2008, **134**, 502.
27 M. G. Manera, G. Leo, M. L. Curri, R. Comparelli, R. Rella, A. Agostiano and L. Vasanelli, *Sens. Actuators, B*, 2006, **115**, 365.
28 M. M. Hawkeye and M. J. Brett, *J. Vac. Sci. Technol., A*, 2007, **25**, 1317.
29 L. González-García, G. Lozano, A. Barranco, H. Míguez and A. R. González-Elipe, *J. Mater. Chem.*, 2010, **20**, 6408.
30 G. K. Kiema, M. J. Colgan and M. J. Brett, *Sol. Energy Mater. Sol. Cells*, 2005, **85**, 321.
31 K. D. Harris, A. Huzinga and M. J. Brett, *Electrochem. Solid-State Lett.*, 2002, **5**, H27.
32 J. J. Steele, M. T. Taschuk and M. J. Brett, *Sens. Actuators, B*, 2009, **140**, 610.
33 G. Armelles, A. Cebollada, A. García-Martín, J. M. García-Martín, M. U. Gonzáles, J. B. Gonzáles-Diaz, E. Ferreiro-Vila and J. F. Torrado, *J. Opt. A: Pure Appl. Opt.*, 2009, **11**, 114023.
34 V. V. Temnov, G. Armelles, U. Woggon, D. Guzatov, A. Cebollada, A. García-Martín, J. M. García-Martín, T. Thomay, A. Leitensftorfer and R. Bratschitsch, *Nat. Photonics*, 2010, **4**, 107.
35 J. Homola, *Anal. Bioanal. Chem.*, 2003, **377**, 528.
36 S. Brunauer, L. S. Deming, W. E. Deming and E. Teller, *J. Am. Chem. Soc.*, 1940, **62**, 1723.
37 M. J. Brett and M. M. Hawkeye, *Science*, 2008, **319**, 1192.
38 M. G. Manera, P. D. Cozzoli, G. Leo, M. L. Curri, A. Agostiano, L. Vasanelli and R. Rella, *Sens. Actuators, B*, 2007, **126**, 562.
39 M. G. Manera, J. Spadavecchia, D. Buso, C. de Julián Fernández, G. Mattei, A. Martucci, P. Mulvaney, J. Pérez-Juste, R. Rella, L. Vasanelli and P. Mazzoldi, *Sens. Actuators, B*, 2008, **132**, 107.

